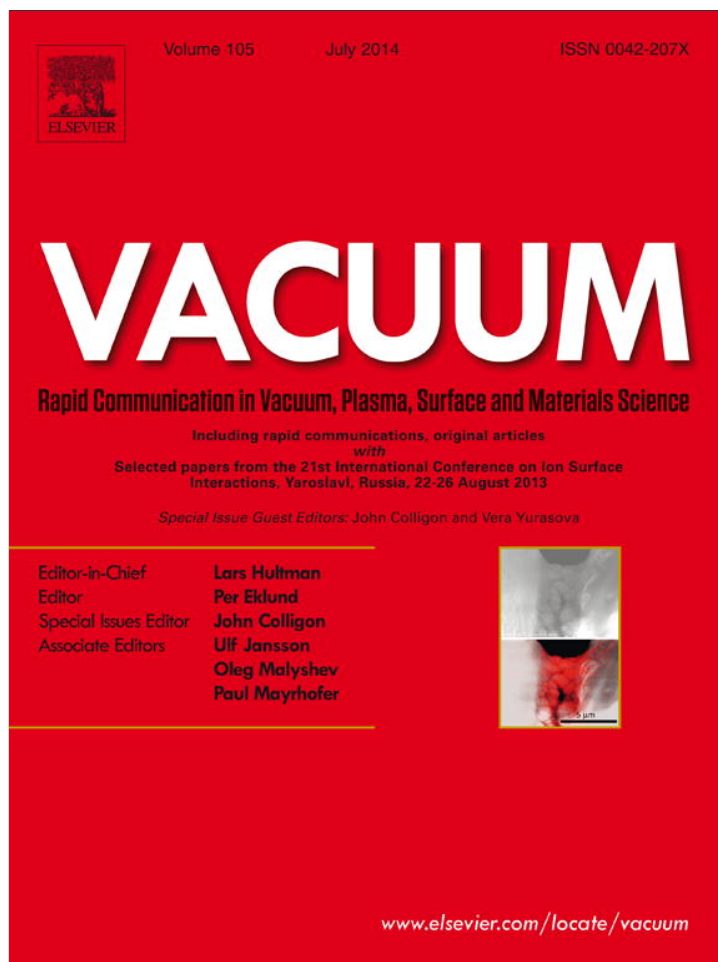


Provided for non-commercial research and education use.
Not for reproduction, distribution or commercial use.



This article appeared in a journal published by Elsevier. The attached copy is furnished to the author for internal non-commercial research and education use, including for instruction at the authors institution and sharing with colleagues.

Other uses, including reproduction and distribution, or selling or licensing copies, or posting to personal, institutional or third party websites are prohibited.

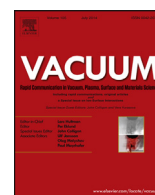
In most cases authors are permitted to post their version of the article (e.g. in Word or Tex form) to their personal website or institutional repository. Authors requiring further information regarding Elsevier's archiving and manuscript policies are encouraged to visit:

<http://www.elsevier.com/authorsrights>



Contents lists available at ScienceDirect

Vacuum

journal homepage: www.elsevier.com/locate/vacuum

Threshold and criterion for ion track etching in SiO₂ layers grown on Si



L.A. Vlasukova^{a,*}, F.F. Komarov^a, V.N. Yuvchenko^a, W. Wesch^b, E. Wendler^b, A.Yu. Didyk^c, V.A. Skuratov^c, S.B. Kislitsin^d

^a Belarusian State University, F. Skorina Ave. 4, 220030 Minsk, Belarus

^b Friedrich-Schiller University Jena, Max-Wien-Platz 1, D-07743 Jena, Germany

^c Laboratory of Nuclear Reactions, Joint Institute for Nuclear Research, Dubna 141980, Russia

^d Institute of Nuclear Physics, National Nuclear Center, Almaty 050032, Kazakhstan

ARTICLE INFO

Article history:

Received 20 September 2013

Received in revised form

8 January 2014

Accepted 10 January 2014

Keywords:

SiO₂/Si

Heavy swift ion

Latent track

Thermal spike model

Nanopores

ABSTRACT

SiO₂ layers thermally grown on Si wafers were irradiated with swift heavy ions in the energy range of (20–710) MeV. Subsequent chemical etching in 4% HF for 6 min produced conical pores with diameters from ~20 to ~80 nm in the SiO₂ layers. We have calculated radii and lifetime of the molten regions in the SiO₂ layers and compared them with the pore diameters and diameter dispersions estimated from scanning electron microscopy and atomic force microscopy. It is shown that the existence of a molten region and its radius can serve as a valid criterion for track “etchability”. In the same etching conditions the etched track diameter and the etching velocity in the track region are proportional to the radius and the lifetime of the molten region.

© 2014 Elsevier Ltd. All rights reserved.

1. Introduction

Swift heavy ion (SHI) irradiation has been of great interest in recent years due to its possibility to tune the material properties. It is possible to modify thin films and nanostructures embedded in solid matrix by means of SHI irradiation. The examples of SHI irradiation assisted modification in thin films are an appearance of room temperature ferromagnetism in ZnO [1], a crystallization of amorphous SnO₂ layers and a formation of regular structures on SnO₂ surface [2,3]. The authors of Refs [4–6] have reported that a shape of Ag, Au, Co nanoparticles changes from spherical to conical or elongated along the SHI beam direction. A possibility of SHI beam induced dissolution and precipitation of Si nanoclusters in silicon nitride and silicon dioxide matrixes is claimed in the recent papers [7,8]. When SHI penetrates a solid, it induces a damaged region called “latent track”. The discovery of ion tracks dates back to 1959 when Silk and Barnes published transmission electron micrographs of mica with long, straight damage trails created by single fragments from the fission of ²³⁵U [9]. Soon after that, it has been realized that ion tracks are narrow (<5 nm), stable, chemically reactive regions which are the result of the interaction of the

projectile ions with the target electrons [10]. Later, it was found that tracks were formed in insulators and badly conducting semiconductors, if the electronic stopping power S_e exceeded a material-dependent threshold value S_{e0} . Owing to a different chemical reactivity of the irradiated regions and the unmodified matrix, nanochannels can be created in track regions by means of treatment in an appropriated etching agent. Integrated into silicon wafers thin nanoporous SiO₂ layers are of special interest for nanotechnology. For instance, in order to create optical devices with the optical confinement of photon crystals [11] or the anti-reflection effect of “moth-eye” [12] it is necessary to improve the insulator’s nanostructuring technique. A combination of lithography and reactive ion etching has been used for the creation of nanostructures in SiO₂ [13,14]. However, the trenches formed by reactive ion etching sometimes have rough sidewalls because of the use of corrosive gases, which can degrade the device characteristics.

A possible solution of this problem may be SHI irradiation of SiO₂ aimed to the “latent tracks” creation. These tracks can be etched in appropriated etchants with the formation of nanochannels [15–18]. Sidewalls of nanochannels etched in the track regions are very smooth as compared to those formed by the reactive ion etching.

In order to govern the etching of latent tracks and achieve a reproducible fabrication of SiO₂ layers with high (up to 10¹¹ cm⁻²)

* Corresponding author. Belarusian State University, Kurchatova Str. 5, Minsk 220108, Belarus. Tel./fax: +375 (17) 398 75 45.

E-mail addresses: vlasukova@bsu.by, ludmila.ulasukova@gmail.com (L.A. Vlasukova).

density of nanochannels with regular shape it is very important to evaluate the crucial factors determining the process of track etching. Amongst these factors a probability of latent track creation along each ion trajectory and a minimum size of a pore which can be etched in the track region are the most important ones. On condition that each swift ion creates latent track the pore density is defined by the ion fluence. Track etching is a threshold process. A commonly used track “etchability” criterion is the threshold electronic stopping power S_{e0} . The corresponding values of S_{e0} vary from 1.5 to 4 keV/nm for SiO₂. Recently, however, the other criterion for “etchability” of tracks was suggested by Dallanora et al. in their interesting paper [16]. The effects of the swift ions passage through SiO₂ and some other insulators are well described using the thermal spike model [19]. The inelastic thermal spike model to calculate the conditions needed to produce an etchable damage in the track region was used in Ref. [16]. The authors of Ref. [16] suggested that the etchable track results from the quenching of a zone which contains the sufficient energy for melting. According to Ref. [16], the track etching appears if the molten region radius is at least 1.6 nm. The homogeneous etching comes out only for the latent track radii larger than 3.0 nm.

On condition that the latent track radii are larger than 3.0 nm and homogeneous etching takes place it can be expected that in the case of more molten region radius the more size of pore can be etched in the track region under the same etching conditions. This suggestion has been proved by the recent experiments [18,20] which have revealed a correlation between the radii of melted regions calculated using the thermal spike model and the sizes of nanopores etched in the track regions of vitreous SiO₂.

In this study, we compared the results of computer simulation of the track formation and the experimental results on the track etching in SiO₂/Si irradiated with SHI in the energy range of (20–710) MeV. Also we tried to elucidate the relation between nanopore’s sizes which were etched in the latent track regions and the track parameters calculated in the frame of the thermal spike model. As compared to a recent experiment limited to scanning electron microscopy (SEM) observations of the etched surfaces [18], here we present the results of atomic force microscopy (AFM) measurements, too.

2. Experimental

The silicon oxide layer of ~ 930 nm thick was thermally grown on the Si (100) wafer. The SiO₂/Si samples of 1×1 cm⁻² were cut from the oxidized Si wafer and irradiated at normal incidence by different ions using three accelerator facilities: a 3 MeV Tandem “Julia” at Jena, Germany (20 MeV Si), an ion cyclotron accelerator DC-60 at Astana, Kazakhstan (92 MeV Kr) and a U400 isochronous cyclotron of the Flerov Laboratory of Nuclear Reactions of the Joint Institute for Nuclear Research at Dubna, Russia (56 MeV Fe, 180 MeV W and 710 MeV Bi). The ion fluence did not exceed 10^9 cm⁻² in all cases. The irradiated samples were treated in a 4% hydrofluoric acid (HF) aqueous solution at room temperature for 6 min. In order to avoid artefacts, all samples were etched in the same etch process. Then, the surface of the etched samples was investigated using the scanning electron microscope Hitachi S-4800 and the atomic force microscope Solver P-47 in the tapping mode. Mean values of the etched pore density, averaged over 3–5 images for each specific irradiation, were obtained both from SEM and AFM images. Moreover, mean values of the etched pore diameter D , averaged over 15–30 tracks for each specific irradiation, were obtained from SEM. Mean values of the pore depth z , averaged over 10–15 tracks, were estimated from AFM profiles. Knowing the pore

depth z , the etching duration t_e , and the etching velocity in the bulk material (V_b), we can determine the etching velocity in the track region (V_t) with the use of the expression $z = (V_t - V_b)t_e$ [21]. The V_b values were calculated from the step height between protected and unprotected regions of the etched virgin sample of SiO₂. The V_b value amounts to 18.3 nm/min. It should be noted that pore depths determined from cross-section TEM or SEM images are more accurate than those determined from AFM images. The last ones may be distorted by the finite size of the probe tip. Though, one can use AFM data for preliminary estimation of V_t .

Our simulations were based on the thermal spike model [19] and the software described in Ref. [18]. The thermophysical parameters of SiO₂ needed for the calculations have been taken from Ref. [16]. In these calculations the radii and lifetimes of the molten regions along swift ion trajectories were determined.

3. Results

The calculated values of the electronic stopping power, radii and lifetimes of the molten regions along swift ion trajectories in SiO₂ are summarized in Table 1. One can see from this Table that in the case of irradiation with 20 MeV Si ions the molten region amounts to 1.5 nm. It nearly coincides with $r = 1.6$ nm reported in Ref. [16] as a threshold value of the melt region radius for the beginning of track etching. For 56 MeV Fe ions this radius amounts to 3.2 nm. It should be noted that according to Ref. [16] the homogeneous etching comes out only for the latent track radii larger than 3.0 nm.

Figs. 1 and 2 show sets of AFM and SEM images of irradiated samples after the etching procedure. For the samples irradiated with 20 MeV Si ions one can see that most of the ion impacts do not result in an etchable track formation and only a few of shallow and slightly defined pits with irregular shape are visible. These structures are hard to estimate quantitatively because they merge with asperities of the surface roughness. Dallanora et al. [16] represented the same pictures of etched SiO₂ surfaces of the samples irradiated with 1–4 MeV Au ions. Because of the low etching efficiency and uncertainty of size and shape of the etched pits it is assumed in Ref. [16] that there is virtually no preferential etching along the tracks. Moreover, for 1–4 MeV Au ions the calculated radius of the molten region does not exceed the threshold value of 1.6 nm. In our case for 20 MeV Si irradiation the calculated value of r is 1.5 nm (see Table 1) that is less than the discussed threshold value. Hence, it should not be expected an appearance of etched tracks for the samples irradiated with 20 MeV Si ions. On the other hand, a distribution of the clearly visible conical pores appears after the etching of samples irradiated with other types of ions (Figs. 1 and 2). The mean values of the etched pore density and size as well as the etching rates in the track region calculated from AFM and SEM images are summarized in Table 2. An analysis of

Table 1
Computer simulation results of the track formation in SiO₂.

Ion type and energy, MeV	S_e , keV/nm (SRIM'2010)	The molten region radius r , nm (Thermal Spike Model)	The molten region lifetime t , ps (Thermal Spike Model)
Si (20 MeV)	3.6	1.5	1.2
Fe (56 MeV)	6.9	3.2	6.7
Kr (92 MeV)	9.2	4.4	12.1
W (180 MeV)	15.8	6.6	28.2
Bi (710 MeV)	23.8	7.8	41.1

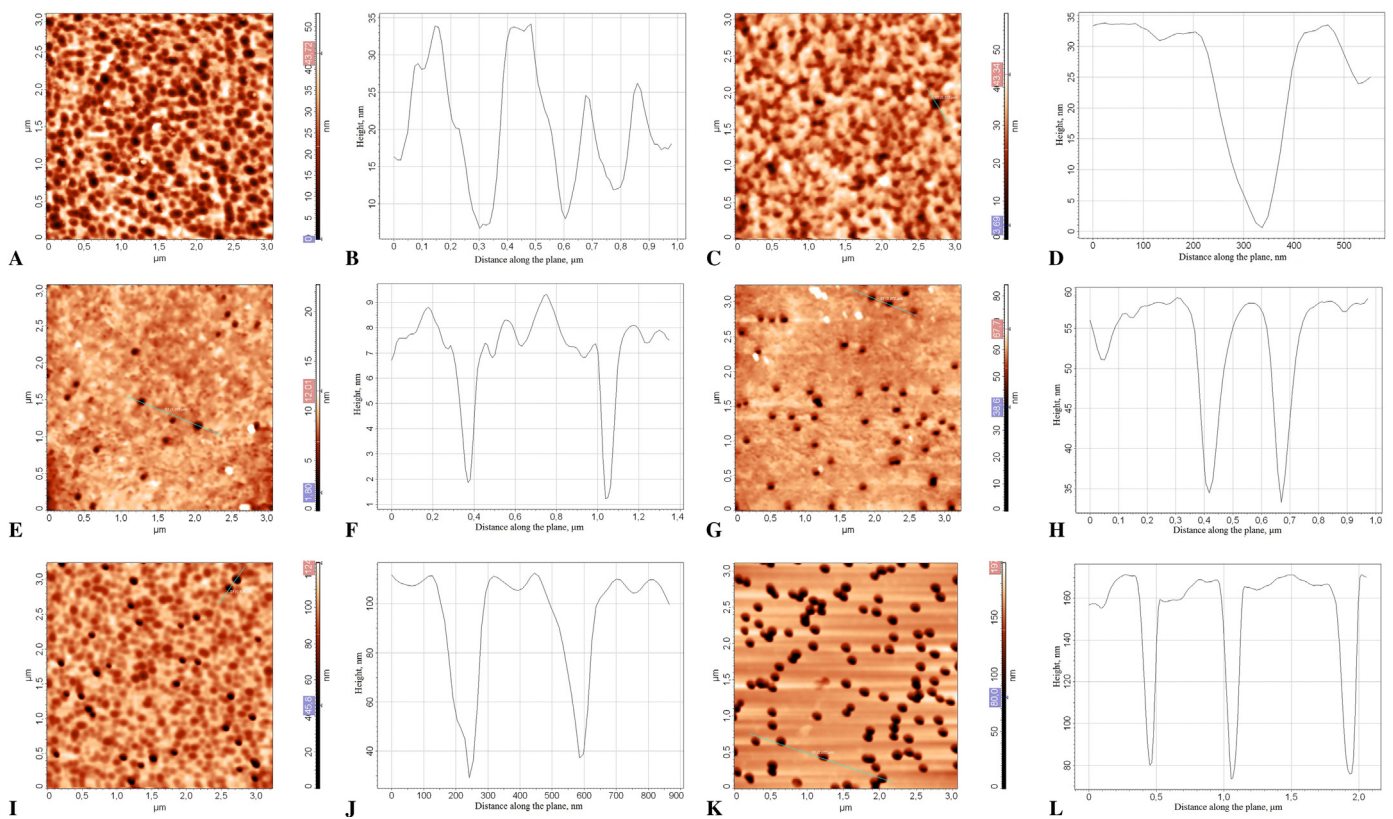


Fig. 1. AFM images and profiles of the etched SiO₂ surfaces: initial sample without irradiation (A, B), the samples irradiated with 20 MeV Si (C, D), 56 MeV Fe (E, F), 92 MeV Kr (G, H), 180 MeV W (I, J) and 710 MeV Bi ions (K, L).

this table shows a reasonable correlation between the fluence and the calculated etched pore densities for all irradiation regimes with the exception of the case of 20 MeV Si. It should be noted that the smallest pore diameter (D nearly 20 nm) and the lowest etching velocity in track region (V_t nearly 19 nm/min) are observed in the case of 56 MeV Fe. For this irradiation regime, the calculated radius of latent track is 3.2 nm. This value is a little bit larger than the threshold one for homogeneous track etching [16]. A comparison between the fluence and the etched pore densities for the samples irradiated with 56 MeV Fe ions shows that practically each ion impact results in the formation of the etched track. It proves a good correlation between our results and the threshold latent track radius for homogeneous track etching predicted in Ref. [16]. Analysis of the data of

Tables 1 and 2 and Figs. 1 and 2 reveals that in the conditions of our experiments such parameters of etched tracks as D and V_t increase with the radius and lifetime of calculated molten regions. It should be noted also the tendency of pore size dispersion decreasing in the row from 56 MeV Fe to 710 MeV Bi. Earlier, for α -SiO₂ samples irradiated with Bi (710 MeV) it was shown that the molten region radius can be used for the estimation of smallest size of the pore which is possible to etch in the track region [22]. In this way, one can forecast the results of track etching (pore density, size and size dispersion) on the base of the molten region radius knowledge. This procedure is of great importance for a choice of proper irradiation regimes aimed to prepare the nanoporous layers with high pore density ($\geq 10^{10}$ cm⁻²) and small pore diameters.

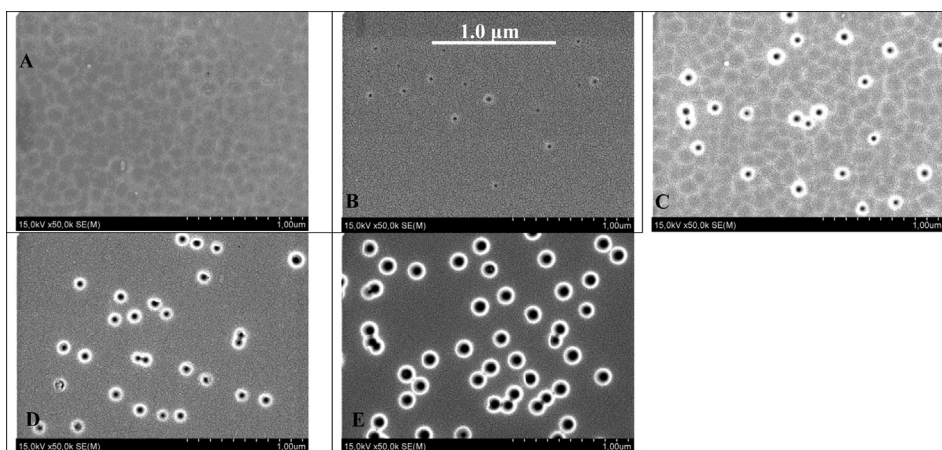


Fig. 2. SEM images of the etched SiO₂ surfaces: the samples irradiated with 20 MeV Si (A), 56 MeV Fe (B), 92 MeV Kr (C), 180 MeV W (D) and 710 MeV Bi ions (E).

Table 2
Irradiation regimes, mean densities and sizes of the etched pores and etching velocities V_t of SiO₂ in the track region.

Ion type and energy	Ion fluence, $\times 10^{-8} \text{ cm}^{-2}$	^a Mean pore density $N_p, \times 10^{-8} \text{ cm}^{-2}$		^b Mean etched pore diameter $D, \text{ nm}$	^c $V_t, \text{ nm/min}$
		SEM data	AFM data		
Si (20 MeV)	3.0 ± 0.23	0.09	0.1	—	—
Fe (56 MeV)	(2–3)	2.15	2.25	22.7 ± 5.1	19.4
Kr (92 MeV)	2.6	3.6	4.8	50.7 ± 10.8	22.1
W (180 MeV)	3	7.4	6.9	52.9 ± 14.0	29.1
Bi (710 MeV)	10	12.2	9.5	82.7 ± 5.6	33.3

^a N was averaged over 3–5 images for each specific irradiation.

^b D was averaged over 15–30 tracks for each specific irradiation.

^c $V_b = 18.3 \text{ nm/min}$. It has been calculated from the step height between the protected and unprotected regions of the etched virgin sample of SiO₂.

4. Conclusions

The etching process of SiO₂ films thermally grown on Si wafers and irradiated with 20 MeV Si, 56 MeV Fe, 92 MeV Kr, 180 MeV W and 710 MeV Bi ions has been investigated and compared with the predictions for track “etchability” based on the thermal spike model [16]. The conical pores with the diameters from ~20 to ~80 nm have been formed in SiO₂ layers irradiated with 56 MeV Fe, 92 MeV Kr, 180 MeV W and 710 MeV Bi ions after the treatment in 4% HF for 6 min. For the samples irradiated with 20 MeV Si the most of ion impacts do not result in an etchable track formation. It has been revealed a good correlation between our results and the threshold melt region radius for the beginning of track etching and for homogeneous track etching predicted in Ref. [16].

It has been shown that the radius of molten region along the swift ion trajectory may be used as a criterion for track “etchability” as well as for the estimation of smallest size of pore which is possible to etch in the track region. In the same etching conditions the etched track diameter and the etching velocity in the track region increase with the radius and lifetime of the calculated molten region. This information is important for a proper choice of irradiation regime aimed to prepare the nanoporous layers with high density ($\geq 10^{10} \text{ cm}^{-2}$) and small size of pores.

Acknowledgements

The study was supported by the Belarusian Republican Foundation for Fundamental Research (Grant T12R-019). The authors are grateful to Dr Liudmila Baran (Belarusian State University) for AFM measurements of the irradiated samples.

References

- [1] Jayalakshmi G, Saravanan K, Balakumar S, Balasubramanian T. *Vacuum* 2013;95:66–70.
- [2] Abhirami KM, Matheswaran P, Gokul B, Sathyamoorthy R, Kanjilal D, Asokan K. *Vacuum* 2013;90:39–43.
- [3] Kumar Y, Herrera M, Singh F, Olive-Méndez SF, Kanjilal D, Kumar Sh, et al. *Mater Sci Eng B* 2012;177:1476–81.
- [4] D’Orleans C, Stoquert JP, Estourne’s C, Cerruti C, Grob JJ, Guille JL, et al. *Phys Rev B* 2003;67:220101-R.
- [5] Singh F, Mohapatra S, Stoquert JP, Avasthi DK, Pivin JC. *Nucl Instr Meth B* 2009;267:936–40.
- [6] Avasthi DK, Mishra YK, Singh F, Stoquert JP. *Nucl Instr Meth B* 2010;268:3027–34.
- [7] Singh SP, Ghosha S, Prakash V, Khan SA, Kanjilal D, Srivastava AK, et al. *Nucl Instr Meth B* 2012;276:51–5.
- [8] Kachurin GA, Cherkova SG, Marina DV, Kesler VG, Volodin VA, Skuratov VA. *Nucl Instr Meth B* 2012;282:68–72.
- [9] Silk ECH, Barnes RS. *Philos Mag* 1959;4:970–2.
- [10] Fleischer RL, Price PB, Walker RM, editors. *Nuclear tracks in solids*. Berkeley: University of California Press; 1975.
- [11] Wang X, Fujimaki M, Awazu K. *Opt Express* 2005;13:1397–486.
- [12] Schultz U, Munzert P, Leitel R, Wendling I, Kaizer N, Tünnerman A. *Opt Express* 2007;15:13108–13.
- [13] Vieillard J, Mazurczyk R, Boum LL, Bouchard A, Chevotot Y, Hannes B, et al. *Microelectron Eng* 2008;85:465–9.
- [14] Norasetthekul S, Park PY, Baik KH, Lee KP, Shin JH, Jeong BS, et al. *Appl Surf Sci* 2001;185:27–32.
- [15] Musket RG, Yoshiyama JM, Contolini J. *J Appl Phys* 2002;91:5760–4.
- [16] Dallanora A, Marcondes DA, Bermudez TL, Fichtner GG, Trautmann C, Toulemonde M, et al. *J Appl Phys* 2008;104:024307.
- [17] Bergamini F, Bianconi M, Cristiani S, Gallerani L, Nubile A, Petriani S, et al. *Nucl Instr Meth B* 2008;266:2475–80.
- [18] Vlasukova LA, Komarov FF, Yuvchenko VN, Mil’chanin OV, Didyk AYU, Skuratov VA, et al. *Bull Russ Acad Sci Phys* 2012;76:582–7.
- [19] Toulemonde M, Dufour C, Meftah A, Paumier E. *Nucl Instr Meth B* 2000;166–167:903–12.
- [20] Nomura K, Ohki Y, Fujimaki M, Wang X, Awazu K. *Nucl Instr Meth B* 2012;272:1–4.
- [21] Spohr K. *Radiat Meas* 2005;40:191–202.
- [22] Komarov FF, Vlasukova LA, Kuchinskyi PV, Didyk AYU, Skuratov VA, Voronova NA. *Lith J Phys* 2009;49:111–5.